Atmospheric Environment 44 (2010) 4024–4034

Contents lists available at ScienceDirect

Atmospheric Environment

journal homepage: www.elsevier.com/locate/atmosenv

An evaluation of the interaction of morning residual layer and afternoon mixed layer ozone in Houston using ozonesonde data

Gary A. Morris [a,*], Bonne Ford [b], Bernhard Rappenglück [c], Anne M. Thompson [d], Ashley Mefferd [e], Fong Ngan [c], Barry Lefer [c]

[a] Dept. of Physics & Astronomy, Valparaiso University, Valparaiso, IN 46383, USA
[b] Dept. of Atmospheric Science, Colorado State University, Ft. Collins, CO 80523, USA
[c] Dept. of Earth and Atmospheric Sciences, University of Houston, Houston, TX 77004, USA
[d] Dept. of Meteorology, The Pennsylvania State University, University Park, PA 16802, USA
[e] Dept. of Land, Air, and Water Resources, University of California, Davis, CA 95616, USA

ARTICLE INFO

Article history:
Received 31 October 2008
Received in revised form
31 May 2009
Accepted 9 June 2009

Keywords:
Ozone
Pollution
Ozonesondes
Boundary layer
Residual layer
TexAQS II
Houston

ABSTRACT

The Tropospheric Ozone Pollution Project (TOPP) launched >220 ozonesondes in Houston (July 2004–June 2008) providing examples of pollution transported into, re-circulated within, and exported from the Houston area. Fifty-one launches occurred during the Texas Air Quality Study (TexAQS) II and the summer portion of IONS-06 (INTEX [Intercontinental Transport Experiment] Ozonesonde Network Study). On 11 days during TexAQS II and on 8 other occasions, ozonesondes were launched both at dawn and in the afternoon. Analysis of these "intensive" launch sequences shows that morning residual layer (RL) ozone concentrations ($[O_3]$) explained 60–70% of the variability found in the afternoon mixed layer (ML). Furthermore, maximum RL $[O_3]$ is nearly identical to the mean ML $[O_3]$ from the previous afternoon (morning minus afternoon $= -1.6 \pm 8.4$ ppbv). During TexAQS II, mean $[O_3]$ below 1.3 km (the mean ML height from ozonesonde data) increased from 37 ± 22 ppbv in the morning to 74 ± 18 ppbv in the afternoon, suggesting an average net local daily O_3 production of ~500–900 tons over the metropolitan Houston area.

1. Introduction

Because exposure to ozone (O_3) leads to numerous health problems, the Environmental Protection Agency (EPA) in 1977 set a National Ambient Air Quality Standard (NAAQS) of a 1-h average <125 ppbv (parts per billion on a volume basis). A more rigorous standard, implemented in 1997, requires the three-year average of the 4th highest daily maximum 8-h average be <85 ppbv. Houston regularly exceeds both standards from March–November, a period longer than most other U.S. metropolitan areas. The EPA recently revised the 8-h standard to 75 ppbv, making it more difficult for Houston to achieve compliance.

A variety of factors contribute to Houston's O_3 pollution. 1) The 4th largest urban population in the U.S., much of which commutes from remote suburbs, results in broad NO_x emissions throughout the Houston–Galveston–Brazoria Region (HGBR, note that Brazoria County is adjacent to Houston and Galveston). 2) One of the largest petrochemical production sectors in the world often produces co-located, concentrated hydrocarbon (HC) and nitrogen oxide (NO_x) emissions, with HC reactivities in the Houston ship channel area 2–5 times higher than those over other U.S. urban locations (Kleiman et al., 2002; Daum et al., 2003). 3) The Parish power plant in Thompsons, TX (<50 km SW of downtown), one of the top 5 U.S. CO_2 emitters (Center for Global Development, 2007), produces NO_x (>5300 tons year^{-1}, 2nd in HGBR, data from the Texas Commission for Environmental Quality, TCEQ). 4) Widespread forests in East Texas are a source of biogenic volatile organic compounds (VOCs). 5) Persistent high pressure and fair weather during summer and a location near Galveston Bay and the Gulf of Mexico frequently lead to stagnant air over the HGBR and/or recirculation of pollution via a land–sea breeze circulation (e.g., Banta et al., 2005). 6) Long-range transport of O_3 and precursors from remote locations can exacerbate local pollution levels (e.g., Pierce et al., 2009).

Past efforts to predict O_3 exceedances in Houston were hampered by the lack of information on the O_3 profile and the extent of vertical mixing (Davis and Speckman, 1999). From July 2004–June 2008, more than 220 ozonesondes were launched from Rice University or the University of Houston (Rice and UH respectively, see Table 1) as part of the Tropospheric Ozone Pollution Project (TOPP) and have provided some of the missing data.

* Corresponding author. Tel.: +1 219 464 5516; fax: +1 219 464 5489.
E-mail address: gary.morris@valpo.edu (G.A. Morris).

1352-2310/$ – see front matter © 2009 Elsevier Ltd. All rights reserved.
doi:10.1016/j.atmosenv.2009.06.057

Table 1
Site information for balloon launches and surface monitors in this study.

Site	Period	Latitude	Longitude
Rice University	7/8/2004–8/3/2006	29.72° N	95.40° W
University of Houston	8/5/2006 – present	29.72° N	95.33° W
CAMS-81	5/3/2000 – present	29.74° N	95.32° W
CAMS-235	10/24/1996 – present	29.67° N	95.13° W
CAMS-411	3/30/2001 – present	29.75° N	95.35° W
CAMS-603	5/16/1998 – present	29.77° N	95.18° W
LaPorte Wind Profiler	7/6/2005 – present	29.70° N	95.10° W

TOPP is the largest O_3 profile data set over a polluted urban area and has been a key component in IONS during the summers of 2004 and 2006 (Thompson et al., 2007). In addition to their use in satellite data validation studies (e.g., Worden et al., 2007; Jiang et al., 2007), the TOPP data have demonstrated the influence of remote forest fires on Houston pollution (Morris et al., 2006; McMillan et al., submitted for publication), found evidence for lightning influence on upper tropospheric O_3 (Cooper et al., 2007), examined the coupling between Mexico City and Houston pollution (Thompson et al., 2008), and linked frontal passages with surface O_3 variations in Houston (Rappenglück et al., 2008).

Most launches occur from 12 to 3 pm local time ("pm" launches) to coincide both with the afternoon O_3 pollution peak and with the ~13:30 local solar time overpass of NASA's Aura satellite (Schoeberl et al., 2006). Some launches occur prior to 11 am local time ("am" launches) on "intensive days," chosen during the 2006 Texas Air Quality (TexAQS) II when high O_3 was forecast but otherwise made without regard to the O_3 forecast. Morning launches allow assessment of the impacts on peak afternoon O_3 concentrations (hereafter, $[O_3]$) of O_3 remaining aloft overnight in a residual layer (RL) that has been transported to Houston or, during stagnant conditions, is a remnant of the previous day's pollution. This paper presents data from 19 "am" launches and 31 "pm" launches occurring on the same or previous afternoon (see Table 2).

Section 2 reviews boundary layer (BL) structure and O_3 data quality. Section 3 outlines our approach to RL and mixed layer (ML) classification. Section 4 describes four case studies that illustrate the role of RL O_3 in high-O_3 events. Finally, Section 5 provides preliminary analyses of the relationships among RL, ML, and surface O_3. Although our data set remains too small and temporally homogenous for firm general conclusions, it nevertheless provides evidence for the utility of soundings in forecasting HGBR O_3.

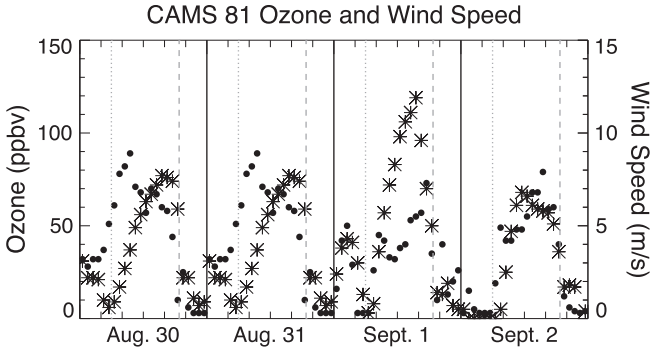

Fig. 1. Data from CAMS-81 (see Table 1) shows increases in surface O_3 at night during periods of higher surface wind speeds. Eddies near the surface grow with the wind speed, entraining material from the residual layer (RL) aloft. The Figure shows surface $[O_3]$ (asterisks) and wind speeds (dots) as well as local sunrises (gray dott-dash lines) and sunsets (gray dashed lines). The solid black vertical lines are at midnight. All data are plotted on Central Standard Time.

2. Background

2.1. Meteorology

With sunset solar heating of the ground ceases, turbulence decays, the surface layer rapidly decouples from air aloft, and radiational cooling at the surface leads to the formation of a stable nocturnal boundary layer (NBL) a few hundred meters thick (Stull, 1988). The quick collapse of the ML after sunset traps O_3 in an RL that can remain intact overnight. O_3 in the NBL is lost through NO titration and surface deposition processes (Zhang and Rao, 1999), which in Houston can result in near total loss by dawn. RL isolation from the NBL is strongest with clear skies and weak, non-turbulent surface winds, conditions often found in post-frontal regions or areas with anticyclonic influences (Chung, 1977).

Fig. 1 depicts an example of the impact of RL O_3 on the NBL during the period 30 Aug.–3 Sept. 2006 with data from the Continuous Air Monitoring System #81 (CAMS-81, see Table 1, data courtesy of TCEQ) near downtown Houston. A front passed through Houston on 29 Aug. (see Rappenglück et al., 2008; Day et al., 2009 for detailed meteorological analyses). On both the 30th and 31st, $[O_3]$ drops to <10 ppbv just before midnight as the hourly mean wind speeds drop to <1 m s^{-1}; just after midnight, wind speeds increase to 3–6 m s^{-1} and $[O_3]$ increases to >20 and >40 ppbv through downward mixing of RL O_3 by eddies. The night of 1 Sept.,

Table 2
Launch data for the 50 launches included in this study. Residual layer (RL) heights are provided for "am" launches while mixed layer (ML) heights are provided for "pm" launches. "X" indicates that a determination of RL or ML height was not possible.

Date	Launch time (GMT)	Burst altitude (km)	RL/ML height (km)	Date	Launch time (GMT)	Burst altitude (km)	RL/ML height (km)
2004/07/29	17:15	24.6	1.3	2006/09/19	18:01	27.9	1.0
2004/07/30	11:45	23.4	1.3	2006/09/20	12:03; 18:01	26.8; 27.9	1.1; 1.2
2004/08/04	19:00	22.1	1.7	2006/09/25	12:00; 18:03	27.2; 27.2	0.8; 1.0
2004/08/05	12:00; 19:00	23.0; 24.1	1.3; 2.0	2006/09/26	15:40; 19:16	27.3; 27.7	1.2; 1.2
2005/08/02	18:46	24.1	1.3	2006/09/27	18:01	27.0	1.2
2005/08/03	11:40; 19:00	22.5; 23.8	1.0; 1.3	2006/10/05	12:01; 18:02	27.9; 26.8	1.3; 1.3
2006/08/17	12:08; 18:38	29.6; 29.9	1.7; 1.6	2006/11/08	13:52; 19:00	27.1; 27.7	0.8; 0.9
2006/08/30	18:14	28.9	1.3	2006/11/17	13:05; 19:00	27.1; 27.7	1.1; 1.3
2006/08/31	12:01; 18:30	27.0; 27.9	1.0; 1.7	2007/08/10	18:32	22.3	2.0
2006/09/01	18:54	27.9	1.7	2007/08/11	12:06; 18:31	22.6; 24.0	1.3; 1.6
2006/09/02	12:02; 18:38	26.2; 28.1	0.9; 2.1	2008/03/07	19:34	27.9	1.4
2006/09/13	17:45	27.6	0.9	2008/03/08	13:41; 19:25	17.8; 28.7	X; 0.9
2006/09/14	12:05; 18:00	28.5; 27.1	1.8; 1.1	2008/05/22	12:08; 18:41	21.7; 22.0	1.3; 1.2
2006/09/15	12:12; 18:04	28.3; 29.1	X; 1.7	2008/06/13	19:28	22.8	1.2
2006/09/19	18:01	27.9	1.0	2008/06/14	06:54; 13:57; 19:24	21.0; 19.1; 20.3	X; 0.8; 1.2
2006/09/20	12:03; 18:01	26.8; 27.9	1.1; 1.2	2008/06/15	06:43; 12:04; 20:12	20.8; 20.9; 27.9	X; 0.6; 1.8

by contrast, has calm winds and almost no surface O_3 from midnight through dawn.

Houston's geographical location also plays an important role its O_3 pollution. Close to the Gulf of Mexico (~80 km) and Trinity and Galveston Bays (~35 km), Houston meteorology is frequently influenced by a land–sea breeze. The importance of this local atmospheric circulation has been examined in previous studies (e.g., Banta et al., 2005; Darby, 2005), and a good example (1 Sept. 2006) is depicted in a TCEQ animation (TCEQ, 2006).

2.2. Ozonesondes

TOPP O_3 profiles are measured using the electrochemical concentration cell (ECC) type (Komhyr, 1986) En-Sci 2Z ozonesonde instruments with 0.5% buffered KI cathode solution. The Jülich Ozone Sonde Intercomparison Experiment (JOSIE) found biases <5%, a precision of 3–5%, and an accuracy of 5–10% up to 30 km for such sondes (Smit et al., 2007).

Pressure, temperature, and relative humidity (RH) measurements are recorded by Vaisala RS80-15N radiosondes. Flights with global positioning systems (GPS) provide latitude, longitude, altitude, wind speed, and wind direction data. Pressure readings are validated through comparisons of pressure altitude with GPS altitude. For flights without GPS instruments, comparisons are made between pre-launch pressure and surface pressure readings at KHOU (Table 1) or from the Kestral 4500 portable weather station (accuracy quoted at 1.5 hPa, www.kestralmeters.com). When pressure offsets are observed, they are usually <2 hPa, meaning that tropospheric O_3 mixing ratios are adjusted <~2% (<~0.2% at the surface).

Fig. 2 shows a comparison of pre-launch ozonesonde readings from the 50 flights in this study with two nearby CAMS sites (see Tables 1 and 3) and the University of Houston Moody Tower (UHMT, located 0.75 km south of the launch site). Hourly CAMS data are interpolated to the launch time. One-minute resolution UHMT [O_3] data are averaged over the 10 min around launch time for comparison with mean ozonesonde data between 85 m a.s.l. (the top of the UHMT) and 210 m a.s.l. (to account for the 20–25 s ozonesonde response time). Fig. 2 also shows a comparison between the readings at the two CAMS stations (~4 km apart) to evaluate geographic variability in Houston. Regression analyses of the relationships between these variables appear in Table 4. Both CAMS sites and the UHMT site show excellent agreement with the ozonesonde readings: all comparisons yield correlation coefficients >0.97 with slopes of nearly 1.00, consistent with Morris et al. (2006). Differences between the sondes and the CAMS sites can be explained by temporal and spatial variability of O_3 in the HGBR.

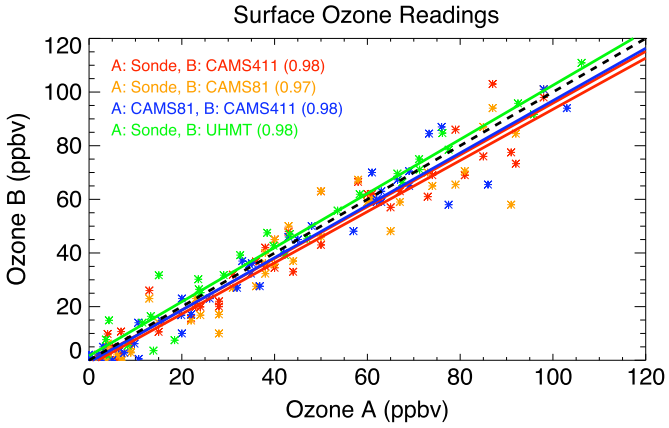

Fig. 2. Comparison of sonde pre-launch O_3 observations with CAMS-81 and CAMS-411 (see Table 1) stations at the time of launch. The legend provides the correlation coefficients for each relationship.

Table 3
Distances between measurement sites in kilometers.

	Rice	UH	CAMS-81	CAMS-411
Rice	–	6.8	8.4	6.3
UH	6.8	–	3.9	4.0
CAMS-81	8.4	3.9	–	3.9
CAMS-411	6.3	4.0	3.9	–

3. Methodology

3.1. Mixed layer height identification

In the morning, solar heating generates turbulent eddies that blend the NBL upwards, forming an ML that by early afternoon is 1–2 km deep (Stull, 1988). Conserved and quasi-conserved trace species (like O_3) are well mixed, and potential temperatures (θ) show constant values in the ML. The entrainment zone (EZ) sits above the ML and serves as the boundary between the turbulent ML below and the non-turbulent lower free troposphere (LFT) above.

Determining the depth and evolution of the ML and its impact on air pollution can be complicated (e.g., Berman et al., 1997). Instead of lidar data or wind profiler data (e.g., Davis et al., 2000; Cohn and Angevine, 2000; Grimsdell and Angevine, 1998), we use 4 sonde variables to assess ML heights in this study (similar to Day et al., 2009). First, a temperature inversion that traps pollution in the daytime ML occurs in the EZ. Second, θ is nearly constant in a well-mixed BL. Nielsen-Gammon et al. (2008) use microwave temperature profiler data to suggest an ML height defined as the minimum height at which θ is 1.5 K greater than its minimum value. Third, a sharp decrease in RH frequently marks the top of the ML (even on cloud-free days) as the sonde enters the drier LFT from the EZ (Stull, 1988). Nielsen-Gammon et al. (2008) suggest the top of the ML is where the dew point first shows a sharp decrease. Fourth, O_3 profiles are strongly linked to the growth of the ML: [O_3] within the ML is nearly constant (Zhang and Rao, 1999), while a sharp [O_3] gradient often occurs at the top of the ML (Athanassiadis et al., 2002). In Houston, a steep negative [O_3] gradient frequently occurs at the top of the ML. Positive gradients suggest the transport of O_3 from remote regions (e.g., Morris et al., 2006). The example of Fig. 3 shows all four variables point to an ML height of ~1.7 km for the pm sounding on 1 Sept. 2006.

3.2. Residual layer identification

The top of the RL, much like the daytime ML, is marked by a capping inversion and sharp RH gradients, while the RL itself

Table 4
Regression fits and correlation coefficients for the relationship of the hourly averaged O_3 concentrations measured at CAMS-81 and CAMS-411 to the pre-launch O_3 measured by the sonde; the relationship of the 10-min average O_3 measured at the University of Houston Moody Tower (UHMT) at launch to the mean concentration measured by the ozonesonde from 85 to 210 m; and the relationship of the surface hourly averaged O_3 concentrations measured at the two CAMS sites to one another. CAMS comparisons include data from 49 launches while the UHMT comparisons include 32 launches.

Relationship	Slope	Intercept	r
CAMS-411 vs. Sonde	0.96 +/− 0.18	−0.6 +/− 1.2	0.98
CAMS-81 vs. Sonde	0.95 +/− 0.19	−1.8 +/− 1.3	0.97
UHMT vs. Sonde 85–210 m	1.008 +/− 0.036	1.1 +/− 1.8	0.98
CAMS-81 vs. CAMS-411	0.98 +/− 0.17	−0.8 +/− 1.2	0.98

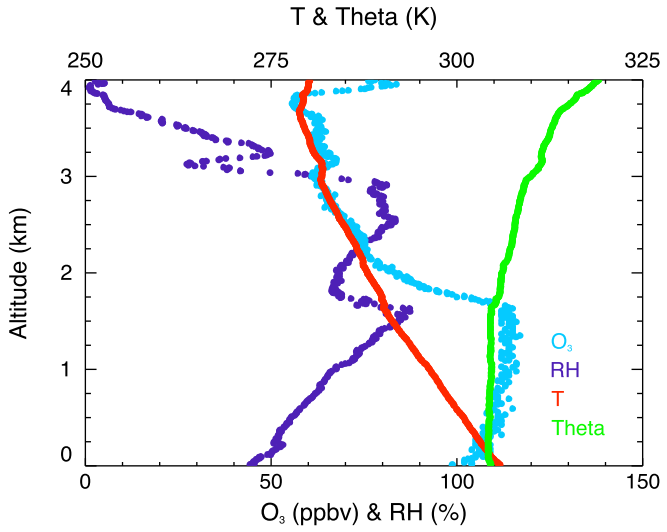

Fig. 3. Example of mixed layer (ML) identification strategy using sonde data from the 1 Sept. 2006 launch at 18:54 GMT (1:54 pm local time). The gradient in the temperature profile shows a notable change at ~1.7 km, while the potential temperature (θ) is nearly constant at ~305 K from the surface up to ~1.7 km. Relative humidity (RH) increases steadily from the surface up to ~1.7 km, at which point a sharp negative gradient appears. The O_3 profile indicates a nearly well-mixed layer from the surface up to 1.7 km, with O_3 > ~100 ppb at the surface, increasing to 110–115 ppb from 0.5 km to 1.7 km, then decreasing sharply at 1.7 km.

often retains properties of the prior day's ML (e.g., [O_3]), with nearly constant θ. Fig. 4 shows an example for an am sounding on 5 Aug. 2004. The base of the RL is found near 0.5 km (as indicated by the temperature, θ, RH, and O_3 data). More difficult to define, the top of the RL likely is just above 1.5 km where the temperature profile shows an inversion, the RH drops off sharply, and [O_3] reaches values that remain nearly constant up to ~4.0 km. Complicating this identification is the fact that [O_3] within the RL often shows variability due to wind shear and horizontal [O_3] gradients.

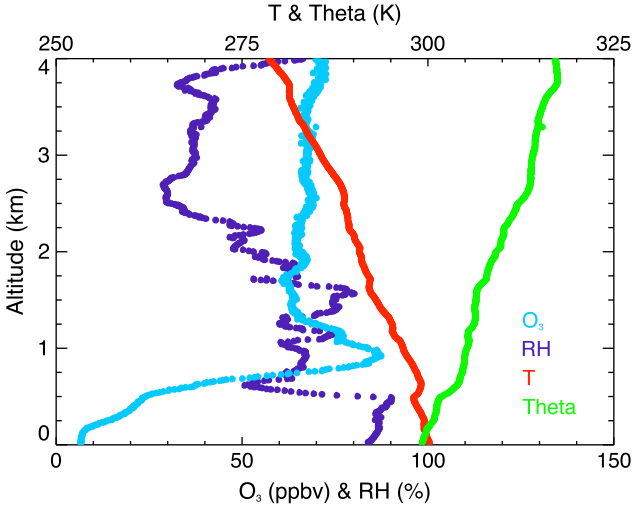

Fig. 4. Example of RL identification strategy using sonde data from 5 Aug. 2004 launch at 12:00 GMT (7:00 am local time). The base of the RL is found just above 0.5 km, where the temperature profile reveals an inversion and the vertical gradient in θ noticeably increases. RH shows a sharp decrease at the same level while ozone increases rapidly. The top of the RL is just below 1.5 km where ozone concentrations reach values that remain nearly constant up to 4.0 km. The temperature profile suggests another inversion (although somewhat weaker than the one at the bottom of the RL) at this level as well. Near the surface, pre-dawn O_3 concentrations are near zero due to NO titration and dry deposition.

3.3. Other resources

Three additional tools aid in ozonesonde data analysis. First, data from the radar wind profiler at the LaPorte Municipal Airport (Table 1, courtesy TCEQ, see Day et al., 2009) are used to identify stagnant conditions. Second, surface analyses from Unisys (weather.unisys.com) provide meteorological context. Third, 24-h back trajectories from three models aid in identifying air mass origins: 1) NOAA's HYSPLIT model (Draxler and Rolph, 2003; graphical output described by Rolph, 2003) is run using the Eta Data Assimilation System with 40-km resolution (EDAS40); 2) the UH Regional Data Assimilation System (UH-RDAS), in which the National Centers for Environmental Prediction (NCEP) North America Mesoscale Model (NAM) in coarse domain is interpolated to 12-km and 4-km resolution, then adjusted by observations using the objective analysis module in the Fifth Generation Mesoscale Model (MM5) (Grell et al., 1994), hereafter referred to as the CMAQ (Community Multiscale Air Quality) trajectories (Byun et al., 2004). (The CMAQ and HYSPLIT trajectories, therefore, are not completely independent since they use the same base model for their winds); and 3) the wind profiler trajectory tool (WPTT, White et al., 2006) which uses hourly data from wind profilers in SE Texas to compute trajectories at fixed altitudes.

4. Case studies

We examine 4 case studies showing the influence of the RL on the ML in the HGBR: 4–5 Aug. 2004, 1–2 Sept. 2006, 5 Oct. 2006, and 10–11 Aug. 2007.

4.1. Case study #1: 4–5 Aug. 2004

Fig. 5 shows O_3 profiles from this three-launch sequence. Ozonesondes in 2004 do not have GPS winds, and the LaPorte wind profiler was not operating, so Fig. 6 shows winds from the Goddard Earth Observing System version 4 (GEOS-4) model (Bloom et al., 2005) interpolated to the ozonesonde profiles. Wind speeds in the HGBR during this 2-day period were <5 m s^{-1} below 1.7 km with a minimum <1 m s^{-1} at ~1.0 km on the morning of 5 Aug.

The 4 Aug. pm data (Fig. 5) indicate a ~1.5 km ML depth with peak [O_3] > 95 ppbv. The 5 Aug. am data show a distinct RL from 0.6 to 1.3 km, with a peak [O_3] > 85 ppbv. The HYSPLIT and CMAQ back trajectories for the air mass sampled at 0.5-km in the am sounding are nearly identical and show the air mass over the Gulf of Mexico 12 h previously (Fig. 7), likely bringing cleaner air in the NBL into the HGBR overnight. In the middle of the RL, however, stagnant winds

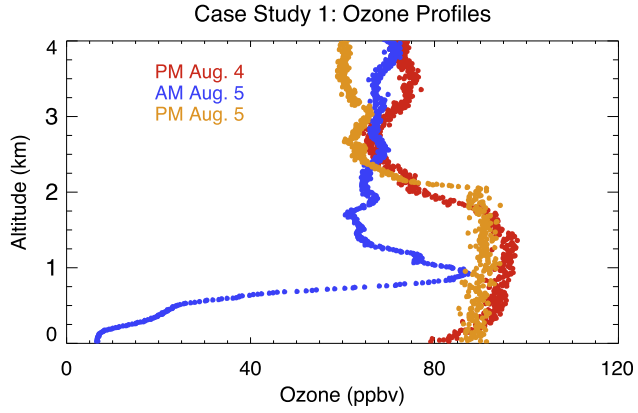

Fig. 5. Ozone profiles from the 3 flights 4–5 Aug. 2004.

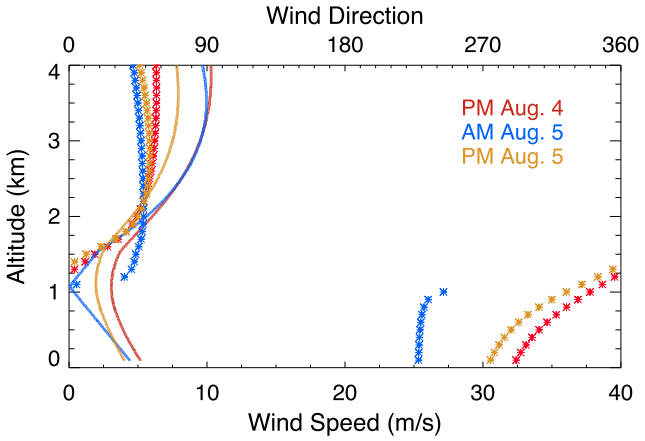

Fig. 6. Wind speeds/directions for 4–5 Aug. 2004 case study using GEOS-4 data interpolated onto sonde profiles. In the Figure, the wind speeds are given by the solid curves while the wind directions are given by the asterisks.

prevailed, as indicated by both the GEOS-4 wind speed profile at 1 km (Fig. 6) and the HYSPLIT 1.25-km back trajectory, which shows air mass recirculation over the HGBR for the previous 24 h (Fig. 7). (Note that this 1.25-km back trajectory suggests that stagnant air was present in a vertical layer near that altitude – inherent uncertainties in trajectories make the exact determination impossible. The appearance of the O_3 peak at ~0.9 km, therefore, is consistent with the stagnant layer predicted by the trajectory model.)

Afternoon ML O_3 on 5 Aug. peaked at ~90 ppbv in an ML ~2.1 km deep. The 0.5-km HYSPLIT back trajectory indicates air

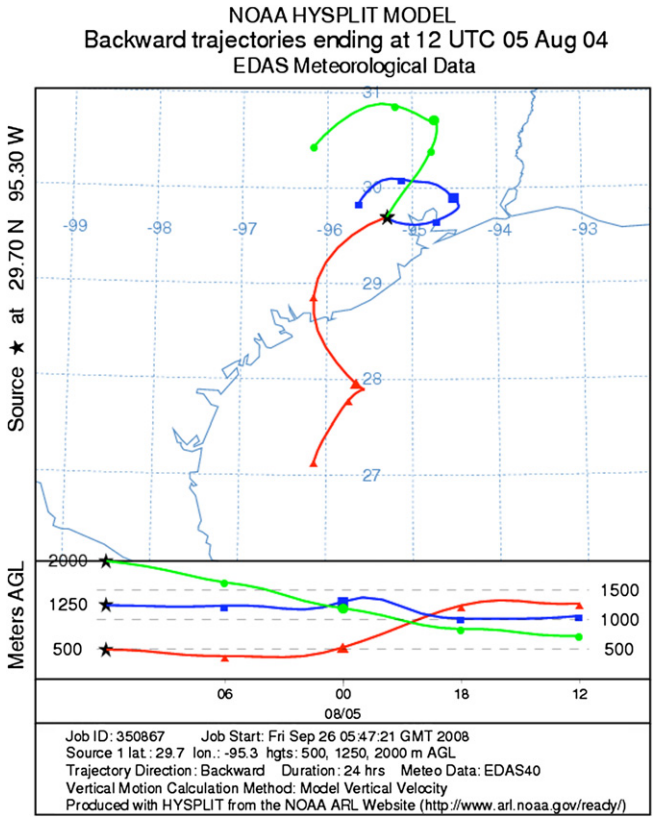

Fig. 7. HYSPLIT 24-h back trajectories for the am flight on 5 Aug. The pm flights on 4 and 5 Aug. show similar behavior below 2 km. Figure courtesy NOAA Air Resources Laboratory (Rolph, 2003).

mass origins along the Texas Gulf Coast SW of Houston, while the 2-km trajectory was over east central Texas 24 h previously (not shown). The 1.25-km trajectory, however, remained within the HGBR for the entire 24-h period. Thus, polluted air from 4 Aug. likely remained in the RL over the HGBR overnight, became re-entrained in the ML on 5 Aug., and contributed to the high O_3 seen in the HGBR on the afternoon of 5 Aug.

4.2. Case study #2: 1–2 Sept. 2006

This period is the subject of several studies (e.g., Day et al., 2009; McMillan et al., submitted for publication; Pierce et al., 2009). After a cold front passed through the HGBR on 29 Aug. 2006, winds shifted from SW to W to N, and background O_3 transported into the HGBR increased by ~30 ppbv (Rappenglück et al., 2008). Subsidence and generally fair weather behind the cold frontal passage provide ideal conditions for further O_3 production. The subsequent three-day period saw "elevated" to "unhealthy" surface O_3 in the HGBR.

Fig. 8 shows the mean of the 8-h ozone maxima from the ~40 operating CAMS sites in the HGBR (hereafter referred to as the 8-h mean) for the period of 26 Aug.–5 Sept. 2006. The maximum 8-h average surface O_3 at 11 CAMS sites in the HGBR exceeded 100 ppbv on 1 Sept., peaking at 121 ppbv at Deer Park (CAMS-235, see Table 1), with an 8-h mean for the HGBR of 91 ± 14 ppbv, the highest day in this study. One-hour ozone values reached 161 ppbv at the CAMS-603 site (Table 1) and exceeded 125 ppbv at 10 CAMS sites. Fig. 8 also shows the daily maximum UHMT O_3 and the mean ML O_3 from the pm soundings. All three data sets show a sharp increase in O_3 after the frontal passage.

Fig. 9 shows the O_3 profiles from the three-sonde sequence. O_3 aloft was highest on 1 Sept., peaking at ~115 ppbv in an ML that was ~1.7 km deep. The next morning, the RL had a maximum O_3 of ~65 ppbv near 0.7 km. The decrease in O_3 in this RL from the previous day may be the result of sporadic rain events that occurred 5–8 pm (CDT) on 1 Sept. (Moody Tower rain gauge data and www.wunderground.com: KHOU station report).

The LaPorte wind profiler observed a layer of weak winds, generally $<$~2.5 m s^{-1}, from 0.5 to 1.5 km altitude between the launches, with stagnant winds in a layer at ~0.6 km at 07:00 and at ~1.1 km by 12:00 GMT, the am launch time on 2 Sept. (see Fig. 10). GPS data from the ozonesonde indicate wind speeds $<$2.5 m s^{-1} in the lowest 1.0 km, with winds $<$1.25 m s^{-1} at 1.0 km (not shown). Below this stagnant layer, winds turned clockwise from SE to S to

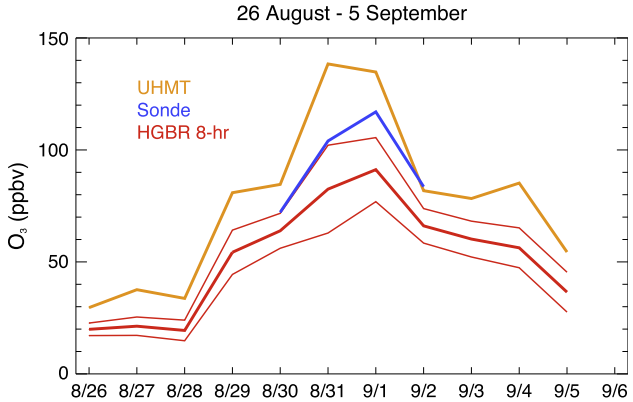

Fig. 8. Mean (thick) and mean ± one standard deviation (thin) 8-h ozone concentrations from the ~40 operating CAMS sites in the HGBR for the period 26 Aug.–5 Sept. 2006. The daily maximum [O_3] at the University of Houston Moody Tower (UHMT) and the maximum ML O_3 from the ozonesondes are also shown. A cold front passed through the HGBR on 29 Sept.

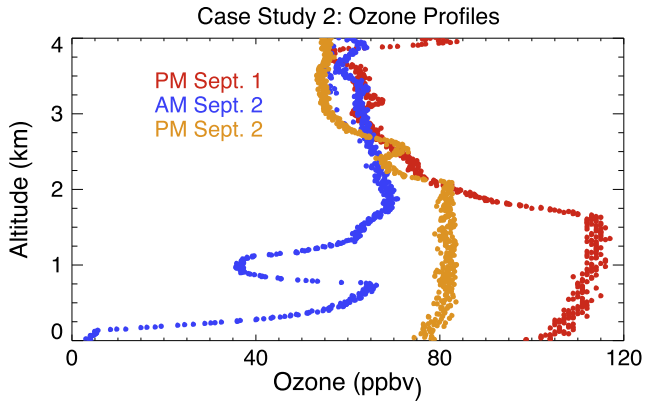

Fig. 9. Ozone profiles from the 3 flights of 1–2 Sept. 2006. The highest O_3 concentrations on the afternoon of 1 Sept. are correspond with the most stagnant air (back trajectory data show air remaining within HGBR).

W, bringing in cleaner air from the Gulf of Mexico during the evening. Just above the layer, flow was NE to E overnight, with stronger winds (>12.5 m s^{-1}) aloft.

HYSPLIT back trajectories for the morning of 2 Sept. show that below 0.5 km, air arrived from the SW from just off Galveston coast 18–24 h earlier. Above 0.5 km, air comes from the E, with higher-level air masses (0.75 and 1.0 km) in Arkansas 24 h prior. Near 0.5 km, where the [O_3] maximum in the dawn RL is found and stagnation is shown by the LaPorte profiler overnight, both the HYSPLIT and CMAQ trajectories show the air remaining in the HGBR for the entire previous 24-h. (The re-circulating layer is seen at ~0.75 km by the WPTT.) The importance of re-circulated O_3 in this event also can be seen in the TCEQ animation (TCEQ, 2006). The air mass with low O_3 near 1.0 km passed through the petrochemical/industrial sector along Galveston Bay en route to Houston and may represent an artifact of SO_2 interference in the sonde method (Rappenglück et al., 2008).

As the ML grew between the 2 Sept. am and pm launches, entrainment of elevated RL O_3 occurred. The afternoon ML height reached 2.1 km, below which [O_3] is a nearly constant ~80 ppbv. Surface [O_3] measured by the sondes increased from 4 to 74 ppbv in the 6.5 h between launches. The decrease in ML [O_3] from 1 to 2 Sept. may be due in part to higher ML heights and wind speeds that provided a larger mixing volume for Houston's pollution. A more appropriate comparison is the horizontal O_3 flux (OF), which we define as

$$\mathrm{OF} = \left([O_3]_{\mathrm{Hou}} - [O_3]_{\mathrm{back}}\right) \times z_{\mathrm{ML}} \times \bar{v}_{\mathrm{ML}}$$

where $[O_3]_{\mathrm{Hou}}$ is the mean pm ML O_3 in Houston, $[O_3]_{\mathrm{back}}$ is the background O_3, as suggested on these days by the 3–4 km mean [O_3], z_{RL} is the height of the ML and $\bar{v}_{\mathrm{RL}}$ is the mean ML wind speed. Using ozonesonde measurements of all three factors, we find

$$1\ \mathrm{Sept}: (165 \pm 73) \times 10^3 \mathrm{ppbv\ m^2\ s^{-1}}$$

$$2\ \mathrm{Sept}: (210 \pm 130) \times 10^3\ \mathrm{ppbv\ m^2\ s^{-1}}$$

a change of $(50 \pm 150) \times 10^3$ ppbv m^2 s^{-1}. While this result is not statistically significant, such a calculation may be useful for future studies.

To summarize, a number of factors enhanced O_3 in Houston during this event: 1) the cold frontal passage increased background O_3 by changing flow from maritime to continental (Pierce et al., 2009); 2) the higher background interacted with locally generated pollution leading to enhanced surface O_3; 3) generally stagnant winds ~0.7 km allowed at least some of the HGBR pollution to be recycled; and 4) descending air and fair weather behind the cold front provided ideal conditions for local O_3 production for several consecutive days.

4.3. Case study #3: 5 Oct. 2006

This case is shown in Fig. 11, with the am [O_3] <5 ppbv and θ nearly constant (~295 K) below 125 m. From 125 to 600 m, θ

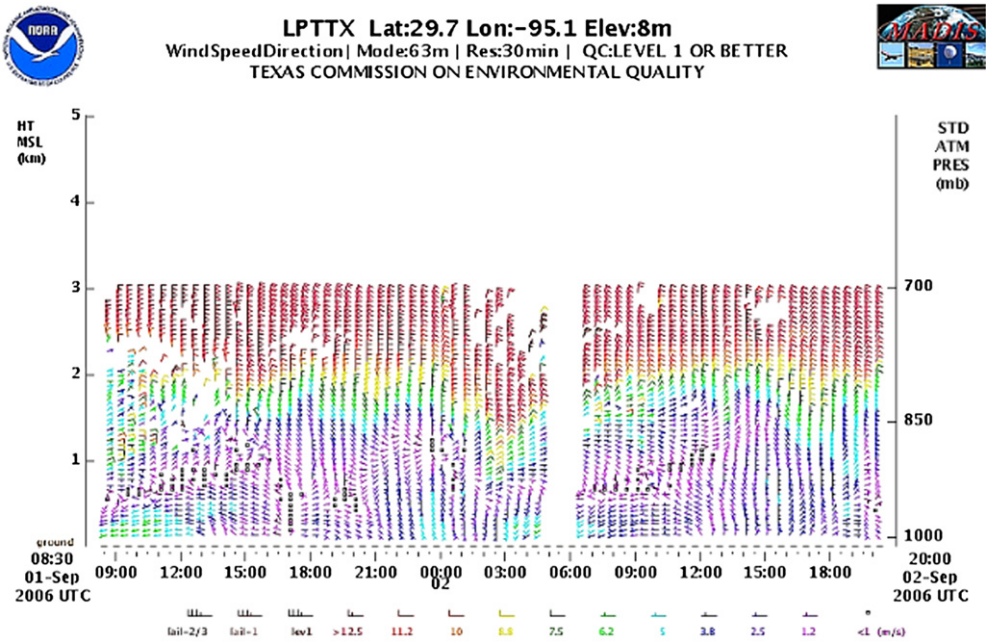

Fig. 10. LaPorte wind profiler data from 1 to 2 Sept. showing generally light (<5 m s^{-1}) winds below 1.5 km, but stronger winds just above the mixed layer as air moves southward behind a cold front that passed through Houston on 29 Aug. Figure courtesy NOAA – Earth System Research Laboratory – Global Systems Division/Meteorological Assimilation Data Ingest System: Cooperative Agency Profiler web site.

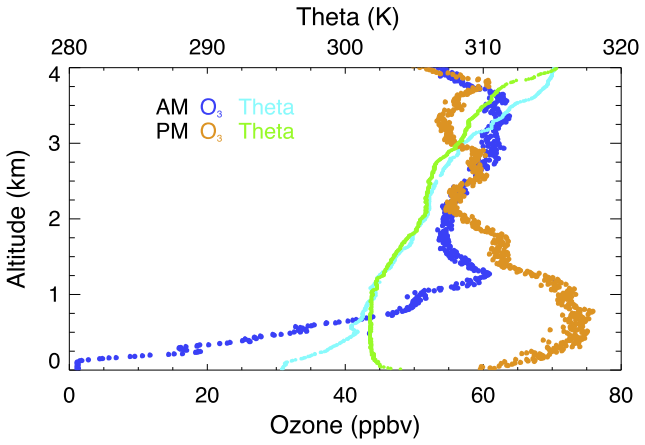

Fig. 11. Ozone (dotted) and θ (solid) profiles from 5 Oct. 2006. The air mass from 1 to 3 km altitude has changed very little between the am and pm launches. The impact of O_3 production in Houston can be seen clearly from the difference between these two profiles. The am RL is found below 1.4 km, peaking at ~60 ppb. The afternoon ML height is about 1.2 km, with O_3 peaking at about 75 ppb. [O_3] from 2.1 to 2.8 km are nearly identical between the morning and afternoon launches. Enhancements from 1.2 to 2.1 km may be due to the interaction of the polluted ML in Houston with the lower free troposphere (LFT), pollution that can be carried to other parts of Texas and beyond.

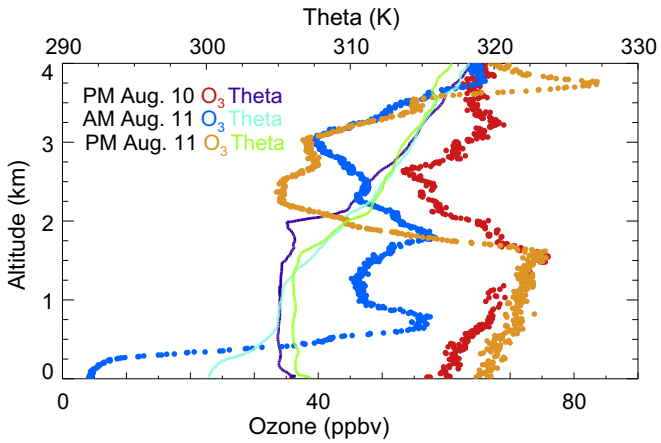

Fig. 13. Ozone (dotted) and θ (solid) profiles for the 10–11 Aug. 2007 3-launch sequence. We see decreasing O_3 aloft (2–3.5 km) with increasing O_3 near the surface. A well-defined RL can be seen in the am profile near 0.8 km, with θ nearly constant values from 0.7 to 1.25 km. On the previous afternoon, θ is constant from 0.15 to 2.0 km, at which point O_3 shows a sharp negative gradient. On the afternoon of the 11th, θ is constant up to 1.7 km, at which point O_3 again shows a sharp negative gradient and nearly the same concentration as the previous afternoon.

increases rapidly up to a negative gradient at ~600 m, marking the RL bottom. [O_3] peaks at ~60 ppbv, then decreases above ~1.3 km, the RL top. TCEQ data indicate the maximum 8-h O_3 on 4 Oct. was 81 ppbv with an 8-hr mean of 53 ± 11 ppbv, consistent with the peak morning RL [O_3]. The pm [O_3] is nearly constant at ~73 ppbv from 0.3 to 1.2 km (the latter being the ML top) with nearly constant θ below (~305 K) and steadily increasing θ above 1.2 km.

LaPorte wind profiler data between the am and pm launches shows persistently light but increasing wind speeds (<2.5 m s^{-1} before 15:00 GMT increasing to 5 m s^{-1} by 16:30 GMT, not shown) <1 km with evening winds on 4 Oct. SE off the Gulf of Mexico and morning winds on 5 Oct. NE, a typical land-sea breeze circulation for Houston. HYSPLIT and CMAQ back trajectories for both soundings show air arriving in the HGBR from East Central Texas and/or Central Louisiana 24 h earlier (not shown). The WPTT shows more Gulf influences for the am sounding and transport from the Beaumont–Port Arthur region (BPAR) 24 h previously near 500 m for the pm sounding (not shown).

4.4. Case study #4: 10–11 Aug. 2007

High pressure over the Gulf of Mexico resulted in several successive days of fair weather and light winds, creating conditions favorable to the recirculation of the Houston plume. LaPorte wind profiler data for this period (Fig. 12) indicate persistent light winds below 2 km, with a layer of winds generally <2.5 m s^{-1} from 0.5 to

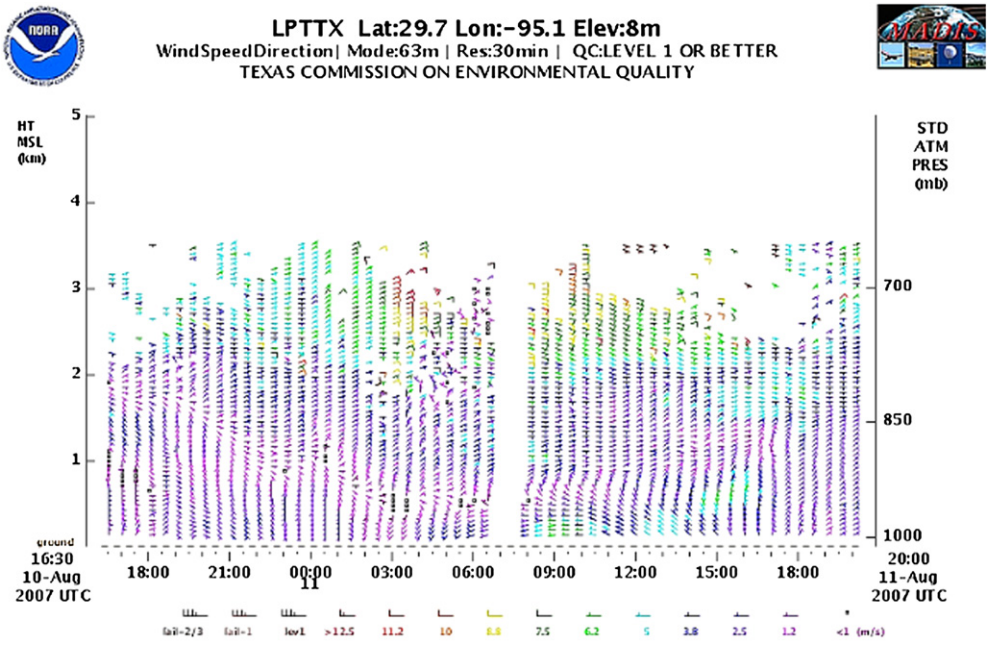

Fig. 12. LaPorte wind profiler data from 10 to 11 Aug 2007. show generally light winds (<5 m s^{-1}) below 2 km. Figure courtesy NOAA – Earth System Research Laboratory – Global Systems Division/Meteorological Assimilation Data Ingest System: Cooperative Agency Profiler web site.

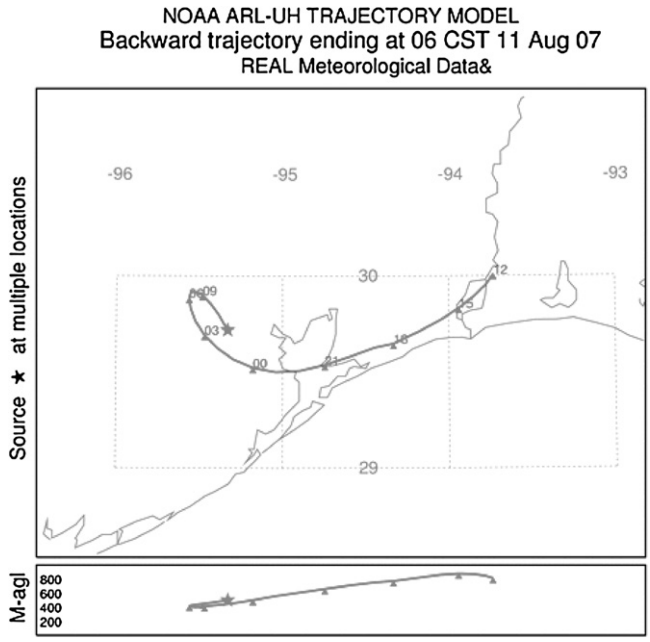

Fig. 14. CMAQ 24-hour back trajectory ending at 500 m over Houston at 6 am on 11 Aug. 2007. The hour markers next to the tick marks along the trajectory are GMT. See text for further details.

1.0 km from the afternoon of 10 Aug. to the afternoon of 11 Aug. The turning of the winds in the lowest 500 m is evidence of the land-sea breeze circulation.

Fig. 13 shows the O_3 and θ for the three launches. The 10 Aug. pm ML is ~2.0 km thick, with nearly constant θ (~305 K). [O_3] in the ML increases steadily from the surface (~60 ppbv) to 1.6 km (~75 ppbv), then decreases slightly up to the ML top (60–65 ppbv) where air with less O_3 may be entrained from the LFT.

The 11 Aug. am RL is well defined by θ, with nearly constant values (~305 K) from 0.6 to 1.3 km. Morning RL [O_3] peaked at 58 ppbv near 0.75 km. The 11 Aug. pm θ shows a well-defined ML, with nearly constant values (~307 K) up to 1.7 km. Afternoon O_3 peaks at ~75 ppbv near 1.6 km, as on the previous afternoon.

GPS wind data from the ozonesondes (not shown) indicate weak and variable winds throughout the ML on both pm launches, with E winds aloft below 4 km. For the am sounding, WNW winds in the boundary layer (<400 m) increased with altitude up to a peak of ~8 m s^{-1} at 250 m; in the RL, N winds were <5 m s^{-1}. From 1.0 to 1.75 km, winds were light (<5 m s^{-1}) and variable, while above 2 km, E winds were 5–10 m s^{-1}.

Both pm launches occurred at ~1:30 pm local time, with surface O_3 only marginally higher on the 11th (~65 ppbv) than on the 10th (~60 ppbv). As with the pm profile on the 10th, O_3 steadily increased from the surface to the top of the ML, where the two profiles are nearly identical. O_3 in the LFT (2–3 km) decreased (10th: 55–70 ppbv; 11th: 35–40 ppbv).

The pm 10 Aug. trajectories (all models) arrived in the HGBR after moving W across the Louisiana Gulf Coast and SE Texas, introducing elevated continental O_3 background values. The pm WPTT back trajectory at 2.0 km for 11 Aug. shows an air mass that arrived in the HGBR via the Gulf of Mexico, potentially resulting in the advection of lower [O_3]. The 0.5-km CMAQ trajectory (Fig. 14) moved from the BPAR along the Texas Gulf Coast, across Galveston Bay, and into Houston through Galveston Bay by the am launch on 11 Aug., suggesting a possible influence of the Beaumont plume on Houston for 11 Aug. The 8-h mean of the surface O_3 monitors in the BPAR on 11 Aug. was 60.6 ± 3.4 ppbv (TCEQ data), consistent with [O_3] at the top of the ML over Houston that day. (The pm 11 Aug. WPTT 0.6–0.9 km trajectories, however, suggests a stagnant air mass over the HGBR rather than a BPAR source.)

5. General analysis

Although the set of 50 soundings in this analysis is relatively small, it still demonstrates the utility of soundings in forecasting O_3. The data suggest that the Houston plume interacts with the LFT and provide an initial assessment of the importance of local production on HGBR O_3.

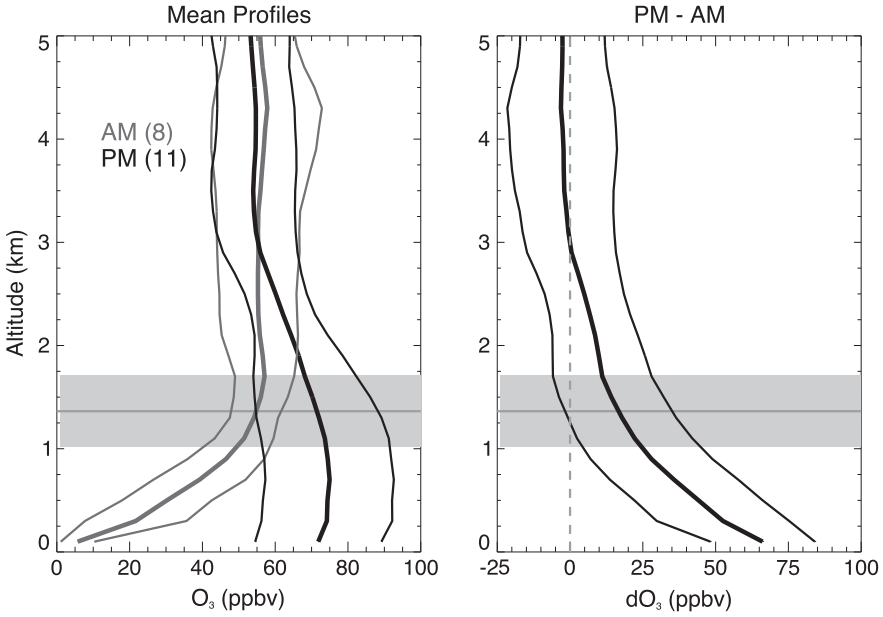

Fig. 15. Mean morning (gray) and afternoon (black) profiles taken during TexAQS II are in the left panel while the mean difference (pm minus am) appears in the right panel. The thick lines represent the means while the thin lines are the mean ±1 standard deviation. The horizontal gray line is the mean mixed layer height (see text) while the surrounding gray shaded area represents one standard deviation.

5.1. Mean profiles during TexAQS II

Fig. 15 summarizes the O_3 profiles from eight am-launches and eleven pm-launches occurring either the same day or the previous afternoon from 17 Aug.–5 Oct. 2006. The mean am [O_3] below 1.3 km (the mean pm ML height) is 37 ± 22 ppbv, while the mean pm [O_3] is 74 ± 18 ppbv, a mean daily enhancement of 37 ± 28 ppbv. Enhancements at the surface are much higher, averaging >65 ppbv.

For the 7 days with both am and pm flights, integrating the am and pm profiles to the top of the pm ML, we find a mean am O_3 column of 4.5 ± 2.3 DU and a mean pm column of 8.2 ± 4.1 DU, an enhancement of 3.7 ± 4.7 DU, consistent with the mixing ratio increases above. Such changes, if assumed to occur in stagnant air over the entire HGBR (with a 40 km radius), result in a mean net daily local O_3 production of ~400 tons. Alternatively, we use the mean wind speed over Houston (4.3 ± 2.9 m s^{-1} from 0.1 to 1.0 km from 23 soundings during TexAQS II) to compute the volume of air in which O_3 production has occurred. This approach yields a mean net local production of ~900 tons. Such O_3 production estimates are reasonable given stationary source emission inventory data (from TCEQ for 2006) of ~160 ton day^{-1} of NO_x in the HGBR and an episodic worst-case estimate of 340 ton day^{-1} of NO_x (all sources in Harris County only; S. Kim, personal communication, 2008).

While the mean am and pm profiles in Fig. 15 agree well above 3 km, enhancements in the pm profile (though not statistically significant) are observed at altitudes of up to ~2.8 km. The highest ML observed by the sondes in this study was 2.1 km on 2 Sept. 2006 (see also Fig. 5d in Thompson et al., 2008), so these enhancements suggest possible export pathways in both the ML and the LFT for Houston pollution. More days with multiple ozonesonde launches are clearly needed to further investigate the impact of the Houston plume on the LFT.

5.2. RL content

Fig. 16 examines the relationship between the maximum RL O_3 in the am soundings and O_3 measured the previous day on the 10 occasions for which the back trajectories from 0.5 to 2.0 km associated with the am launch and those associated with the previous pm launch show similar origins and for which no rainfall was observed between the two launches (2004/07/29–30, 2004/08/04–05; 2006/08/30–31; 2006/09/13–14; 2006/09/19–20, 2006/09/25–26, 2007/08/10–11, 2008/03/07–08, 2008/06/13–14, and 2008/06/14–15). Two data sets are used for comparison: the 8-h mean and the mean ML O_3 observed by the previous pm ozonesondes. Both data sets show a strong correlation with the maximum am RL [O_3] (see Table 5 for statistical data). The mean differences are: (am RL [O_3] – 8-h mean) = 3.2 ± 8.0 ppbv; (am RL [O_3]–pm ML [O_3]) = −1.6 ± 8.4 ppbv.

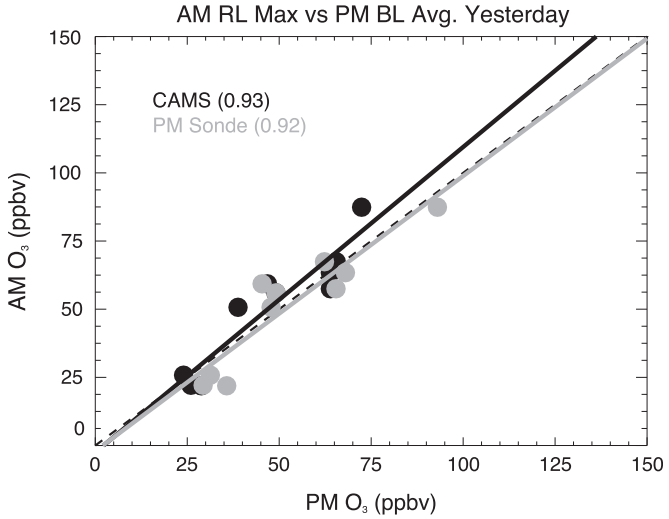

Fig. 16. The relationship between the maximum O_3 in the morning RL and the average ML O_3 from the previous afternoon is shown. Two data sets are used to determine the ML ozone: the dark circles are the mean of the 8-h maximum data from the ~40 CAMS sites in the HGBR. The gray circles are the maxima from the previous afternoon's sounding.

Table 5
Regression fits and correlation coefficients for the relationship of the maximum am RL [O_3] from 10 flights to the pm [O_3] as measured by CAMS surface stations in the HGBR and by the previous afternoon's ozonesonde profile.

Relationship	Slope	Intercept	r
CAMS 8-h mean	1.12 +/− 0.15	−2.5 +/− 7.7	0.93
Sonde ML Average	1.01 +/− 0.15	−2.1 +/− 8.5	0.92

5.3. Impact of RL on afternoon BL

Fig. 17 shows the relationship among three possible predictive variables for pm O_3: 1) The 8-h mean from CAMS data is compared with the maximum RL [O_3] from the same day's am sounding; 2) mean ML [O_3] as determined from the pm sounding is compared with the maximum RL [O_3] from the same day's am sounding; and 3) the 8-h mean from CAMS is compared to its value from the previous day. The statistical data in Table 6 indicates that while correlation coefficients are similar, the sounding information results in a slope closer to 1.00. Furthermore, the am RL data explain ~60% of the variability found in the pm data, consistent with Neu et al. (1994), Kleinman et al. (1994), and Millan et al. (2000), all of which suggest that re-entrainment of RL O_3 can account for 50–100% of the day's maximum surface [O_3].

6. Summary and future work

The ozonesonde data presented in this work demonstrate the impact that O_3 stored in the RL overnight can have on HGBR surface

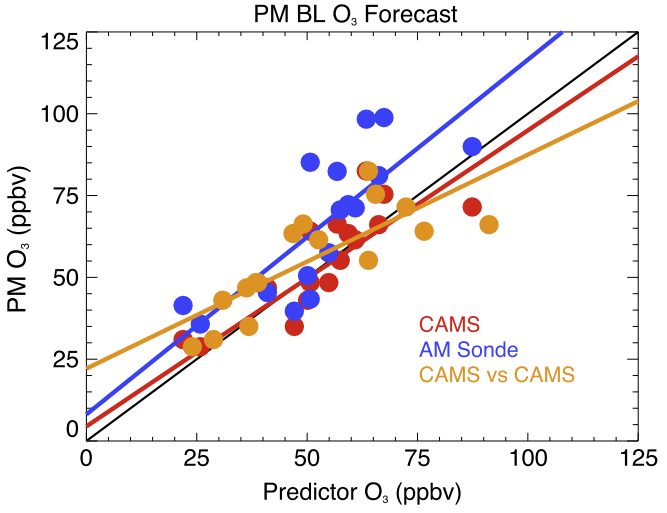

Fig. 17. Three attempts at predicting ML [O_3] are shown. The HGBR mean 8-h O_3 from CAMS is compared to the maximum RL [O_3] from the same day's am sounding (black), and the mean ML [O_3] as determined from the afternoon sounding is compared with the same day's maximum RL [O_3] from the am sounding (dark gray). Finally, today's HGBR mean 8-h ozone from CAMS data is compared with yesterday's (light gray) assuming persistence. While correlation coefficients are similar in all three cases, the sounding information results in a slope closer to 1.00.

Table 6
Regression fits and correlation coefficients for the relationship of the mean pm ozone concentration to several predictor variables. See text for details. Although the correlation coefficients are all similar, the sounding information improves the statistical relationships.

Relationship	Slope	Intercept	*r*
CAMS 8-h mean vs. am sonde RL max	0.84 +/− 0.15	10.2 +/− 8.5	0.83
PM sonde ML avg. vs. am sonde RL max	1.08 +/− 0.23	8 +/− 13	0.78
CAMS today vs. yesterday	0.65 +/− 0.13	22.1 +/− 7.3	0.79

O_3 the following day. A strong correlation was found between the maximum am RL [O_3] with the subsequent afternoon's surface [O_3], the former explaining 60–70% of the latter. Furthermore, the maximum RL [O_3] is consistent with the HGBR 8-h mean [O_3] and the mean pm BL [O_3] from the previous day (absent rain and with similarly back trajectories or a stagnant air mass). Differences between the pm and am profiles from the same day during TexAQS II suggest local production increased ML O_3 from 37 ± 22 ppbv to 74 ± 18 ppbv, a daily enhancement of 37 ± 28 ppbv, or ~400–900 tons of O_3. Data from intensive launch days may be useful for quantifying the O_3 flux out of the HGBR in the ML and in the LFT where it can be transported over great distances and affect air quality in regions remote from Houston. The case studies suggest impacts from pollution transported within Southeast Texas and re-circulated within the HGBR.

Statistically stronger conclusions would be achieved through intensive launches conducted throughout the year, allowing insights into seasonal differences in local O_3 production and transport. Regular am soundings, particularly during the spring and summer high-O_3 seasons, could prove valuable in forecasting afternoon HGBR [O_3].

Acknowledgements

The authors gratefully acknowledge the work of numerous students at Rice, Valparaiso University, and UH: A. Bryan, S. Boudreaux, A. Chow, B. Day, S. Hersey, S. Holcomb, D. Lutz, M. McCormick, B. Morris, L. Pedemonte, R. Perna, R. Tahiri, M. Taylor, E. Thompson, and J. Wright. We also thank the Federal Aviation Administration, particularly David Svedberg, and the staffs at Rice and UH for accommodating our research; the NOAA Air Resources Laboratory for the HYSPLIT transport and dispersion model and the READY web site (http://www.arl.noaa.gov/ready.html); the NOAA Earth System Research Laboratory for the WPTT; and to Bryan Lambeth and Wayne Angevine for the LaPorte wind profiler data. Thanks to Bryan Johnson, Walter Komhyr, and Sam Oltmans for useful discussions, and to Holger Volmel for the STRATO software. Finally, thanks to the anonymous reviewers whose comments substantially enhanced this paper. Initial support for TOPP came from the Shell Center for Sustainability at Rice. TOPP is supported by the Texas Commission for Environmental Quality, the NASA Division of Earth Science Aura Validation Program, and the NASA Tropospheric Chemistry Program (for IONS). This work was completed while the author was funded by a Fulbright Scholar grant.

References

Athanassiadis, G.A., et al., 2002. Boundary layer evolution and its influence on ground level ozone concentrations. Environ. Fluid Mech. 2, 339–357.
Banta, R.M., Senff, C.J., Nielsen-Gammon, J., Darby, L.S., Ryerson, T.B., Alvarez, R.J., Sandberg, S.P., Williams, E.J., Trainer, M., 2005. A bad air day in Houston. Bull. Am. Meteorol. Soc. 86, 657–669.
Berman, S., Ku, J.Y., Zhang, J., Rao, S.T., 1997. Uncertainties in estimating the mixing depth-comparing three mixing depth models with profiler measurements. Atmos. Environ. 31, 3023–3039.
Bloom, S., da Silva, A., Dee, D., Bosilovich, M., Chern, J.-D., Pawson, S., Schubert, S., Sienkiewicz, M., Stajner, I., Tan, W.-W., Wu, M.-L., 2005. Documentation and validation of the Goddard Earth Observing System (GEOS) data assimilation system – version 4, Tech. Report Series on Global Modeling and Data Assimilation 104606, 26.
Byun, D.W., Kim, S.B., Moon, N.K., Ngan, F., Li, Y., Ng, T., 2004. Real-time Trajectory Analysis Operation and Tool Development. HARC Project No: H19.2003.
Center for Global Development, 2007. CGD Ranks CO_2 Emissions from Power Plants Worldwide. http://www.cgdev.org/content/article/detail/14846.
Chung, Y.-S., 1977. Ground-level ozone and regional transport of air pollutants. J. Appl. Meteorol. 16, 1127–1136.
Cohn, S.A., Angevine, W.M., 2000. Boundary layer height and entrainment zone thickness measured by lidars and wind-profiling radars. J. Appl. Meteorol. 39, 1233–1247.
Cooper, O.R., et al., 2007. Evidence for a recurring eastern North America upper tropospheric ozone maximum during summer. J. Geophys. Res. 112, D23304. doi:10.1029/2007JD008710.
Darby, L.S., 2005. Cluster analysis of surface winds in Houston, Texas, and the impact of wind patterns on ozone. J. Appl. Meteorol. 44, 1788–1806.
Davis, J.M., Speckman, P., 1999. A model for predicting maximum and 8 h average ozone in Houston. Atmos. Environ. 33, 2487–2500.
Davis, K.J., Gamage, N., Hagelberg, C.R., Kiemle, C., Lenschow, D.H., Sullivan, P.P., 2000. An objective method for deriving atmospheric structure from airborne lidar observations. J. Atmos. Ocean. Technol. 17, 1455–1468.
Daum, P.H., et al., 2003. A comparative study of O_3 formation in the Houston urban and industrial plumes during the 2000 Texas Air Quality Study. J. Geophys. Res. 108 (D23). doi:10.1029/2003JD003552.
Day, B.M., Rappenglück, B., Clements, C.B., Tucker, S.C., Brewer, W.A., 2009. Nocturnal boundary layer characteristics and land breeze development in Houston, Texas during TexAQS II. Atmos. Environ. 44, 4014–4023.
Draxler, R.R., Rolph, G.D., 2003. HYSPLIT (HYbrid Single-Particle Lagrangian Integrated Trajectory). Model access via NOAA ARL READY. NOAA Air Resources Laboratory, Silver Spring, MD. http://www.arl.noaa.gov/ready/hysplit4.html Website.
Grell, G.A., Dudhia, J., Stauffer, D., 1994. A Description of the Fifth-Generation Penn State/NCAR Mesoscale Model (MM5), NCAR Technical Note: NCAR/TN-398+STR.
Grimsdell, A.W., Angevine, W.M., 1998. Convective boundary layer height measurement with wind profilers and comparison to cloud base. J. Atmos. Ocean. Technol. 15, 1331–1338.
Jiang, Y.B., et al., 2007. Validation of Aura Microwave Limb Sounder ozone by ozonesonde and lidar measurements. J. Geophys. Res. 112, D24S34. doi:10.1029/2007JD008776.
Kleinman, L., Lee, Y.-N., Springston, S.R., Nunnermacker, L., Zhou, X., Brown, R., Hallock, K., Klotz, P., Leahy, D., Lee, J.H., Newman, L., 1994. Ozone formation at a rural site in southeastern United States. J. Geophys. Res. 99, 3469–3492.
Kleiman, L.I., Daum, P.H., Imre, D., Lee, Y.-N., Nunnermacker, L.J., Springston, S.R., Weinstein-Lloyd, J., Rudolph, J., 2002. Ozone production rate and hydrocarbon reactivity in 5 urban areas: a cause of high ozone concentration in Houston. Geophys. Res. Lett. 29 (10), 1467. doi:10.1029/2001GL014569.
Komhyr, W.D., 1986. Operations Handbook: Ozone Measurements to 40 km Altitude with Mode 4A Electrochemical Concentration Cell (ECC) Ozonesondes (Used with 1680-Mhz Radiosondes), NOAA Technical Memorandum ERLARL-149.
McMillan, W.W., Pierce, R.B., Andrews, A., Barnet, C., Evans, K., Fischer, M., Hoff, R., LeferB., Morris, G., Osterman, G., Sparling, L. Satellite observations of moderate range pollution transport contributions to an ozone exceedance episode on 1 September 2006 during TexAQS II. J. Geophys. Res., submitted for publication.
Millan, M., Mantilla, E., Salvador, R., Carratala, A., Sanz, M., Alonso, L., Gangoiti, G., Navazo, M., 2000. Ozone cycles in the Western Mediterranean Basin: interpretation of monitoring data in complex coastal terrain. J. Appl. Meteorol. 39, 487–508.

Morris, G.A., Hersey, S., Thompson, A.M., Cooper, O.R., Stohl, A., Colarco, P.R., McMillan, W.W., Warner, J., Johnson, B.J., Witte, J.C., Kucsera, T.L., Larko, D.E., Oltmans, S.J., 2006. Alaskan and Canadian forest fires exacerbate ozone pollution over Houston, Texas, on 19 and 20 July 2004. J. Geophys. Res. 111, D24S03. doi:10.1029/2006JD007090.

Neu, U., et al., 1994. On the relation between ozone storage in the residual layer and daily variation in near-surface ozone concentration – a case study. Boundary Layer Meteorol. 69, 221–247.

Nielsen-Gammon, J.W., Powell, C.L., Mahoney, M.J., Angevine, W.M., Senff, C., White, A., Berkowitz, C., Doran, C., Knupp, K., 2008. Multisensor estimation of mixing heights over a coastal city. J. Appl. Meteorol. Clim. 47, 27–43.

Pierce, R.B., Al-Saadi, J., Kittaka, C., Schaack, T., Lenzen, A., Bowman, K., Szykman, J., Soja, A., Ryerson, T., Thompson, A.M., Bhartia, P., Morris, G.A., 2009. Impacts of background ozone production on Houston and Dallas, Texas, air quality during the second Texas air quality study field mission. J. Geophys. Res. 114, D00F09. doi:10.1029/2008JD011337.

Rappenglück, B., Perna, R., Zhong, S., Morris, G.A., 2008. An analysis of the vertical structure of the atmosphere and the upper-level meteorology and their impact on surface ozone levels in Houston, TX. J. Geophys. Res. 113, D17315. doi:10.1029/2007JD009745.

Rolph, G.D., 2003. Real-time Environmental Applications and Display sYstem (READY). Website. NOAA Air Resources Laboratory, Silver Spring, MD. http://www.arl.noaa.gov/ready/hysplit4.html.

Schoeberl, M.R., Douglass, A.R., Hilsenrath, E., Bhartia, P.K., Beer, R., Waters, J.W., Gunson, M.R., Froidevaux, L., Gille, J.C., Barnett, J.J., Levelt, P.F., DeCola, P., 2006. Overview of the EOS Aura mission. IEEE Trans. Geosci. Remote Sens. 44 (5), 1066–1074.

Stull, R.B., 1988. An Introduction to Boundary Layer Meteorology. Kluwer Academic.

Smit, H.G., Straeter, W., Johnson, B.J., Oltmans, S.J., Davis, J., Tarasick, D.W., Hoegger, B., Stubi, R., Schmidlin, F.J., Northam, T., Thompson, A.M., Witte, J.C., Boyd, I., Posny, F., 2007. Assessment of the performance of ECC-ozonesondes under quasi-flight conditions in the environmental simulation chamber: insights from the Jülich Ozone Sonde Intercomparison Experiment (JOSIE). J. Geophys. Res. 112, D19306. doi:10.1029/2006JD007308.

TCEQ, 2006. http://www.tceq.state.tx.us/assets/public/compliance/monops/air/sigevents/06/060901ani-houo3.html.

Thompson, A.M., et al., 2007. Intercontinental Transport Ozonesonde Network Study (IONS, 2004): 1. Summertime UT/LS (upper troposphere/lower stratosphere) ozone over northeastern North America. J. Geophys. Res. 112, D12S12. doi:10.1029/2006JD007441.

Thompson, A.M., Yorks, J.E., Miller, S.K., Witte, J.C., Dougherty, K.M., Morris, G.A., Baumgardner, D., Ladino, L., Rappenglück, B., 2008. Free tropospheric ozone sources and wave activity over Mexico City and Houston during MILAGRO/Intercontinental Transport Experiment (INTEX-B) Ozonesonde Network Study, 2006 (IONS-06). Atmos. Chem. Phys. 8, 5113–5125.

White, A.B., Senff, C.J., Keane, A.N., Darby, L.S., Djalalova, I.V., Ruffieux, D.C., White, D.E., Williams, B.J., Goldstein, A.H., 2006. A wind profiler trajectory tool for air quality transport applications. J. Geophys. Res. 111, D23S23. doi:10.1029/2006JD007475.

Worden, H.M., Logan, J.A., Worden, J.R., Beer, R., Bowman, K., Clough, S.A., Eldering, A., Fisher, B.M., Gunson, M.R., Herman, R.L., Kulawick, S.S., Lampel, M.C., Luo, M., Megretskaia, I.A., Osterman, G.B., Shephard, M.W., 2007. Comparisons of Tropspheric Emission Spectrometer (TES) ozone profiles to ozonesondes, methods and initial results. J. Geophys. Res. 112, D03309. doi:10.1029/2006JD007258.

Zhang, J., Rao, S.T., 1999. The role of vertical mixing in the temporal evolution of ground-level ozone concentrations. J. Appl. Meteorol. 38, 1674–1691.